International Journal of Mechanics and Applications 2012, 2(5): 81-87
DOI: 10.5923/j.mechanics.20120205.05

A Combination of a 3 Step Temporal Phase Algorithm and a High Speed Interferometer System for Dynamic Profile Measurements

David Asael Gutiérrez Hernández*, Carlos Pérez López, Fernando Mendoza Santoyo

Centro de Investigaciones en Óptica. Lomas del Bosque 115. Col. Lomas del Campestre. C.P. 31715, León, Guanajuato. México

Abstract This work presents the application of a temporal phase algorithm on a high speed optical interferometry vibration study. The object is a rectangular plate clamped on its four sides. The dynamic event of a complete cycle of vibration is registered by means of a high speed electronic speckle pattern interferometry system (HS ESPI). The HS ESPI system contains a CMOS camera set at 4000 frames per second leaving the shutter widely open all the time. A group of intensity patterns of interference are recorded, different sets of fringe patterns along the cycle of vibration come from the subtraction of the intensity patterns of interference and are processed by a three-frame temporal phase measurement method to recover the phase of deformation of the plate. The result is reported and is also compared with the mechanical phase described on the theory.

Keywords ESPI, High Speed Interferometry, Vibrations

1. Introduction

Optical techniques for vibrations measurements have had a very important role in industrial evolution. The introduction of high speed cameras to very well known systems like electronic speckle interferometry and digital holography gives a big opportunity to study dynamic events with much more precision. High speed optical interferometry is a powerful optical tool for measuring the phase difference between two events of an object under some mechanical change[1, 2]. There are some industrial and biomedical applications that use optical interferometry measurements for vibration analysis, also for testing mechanical objects, and recently for measuring of non solid objects (elastics)[3]. Temporal phase measurement techniques have been used to detect the phase for the study of the complete deformation evolution in static and dynamic events. The optical set ups used in these techniques employed tilted mirrors or piezoelectric components to retrieve the optical phase of the reference beam. In this work we present the use of a known temporal phase measurement algorithm for temporal asynchronous demodulation applied to a sequence of High-Speed Electronic Speckle Pattern Interferometry (HS-ESPI) interferograms from an optical set up that does not have tilting mirrors or piezoelectric component, in this case, the optical phase is obtained because the retrieved optical phase comes from the object beam which is under continuous movement due to an external excitation. The interferograms' sequence comprises a whole cycle of the harmonic event taken from a clamped rectangular metal plate excited at the first resonant frequency. In order to obtain the phase from these interferograms' sequence, the algorithm only needs 3 interferograms taken during various cycles. The High-Speed system works at 4000 fps (frames per second) using a CMOS camera and a continuous wave (cw) Verdi laser at 532 nm. Simulated phase data is compared to experimental results and plotted to show errors in the proposed method.

To determine phase, electronic and analytic techniques are used.. Some of these algorithms have worked with a set of three, four or five recorded fringe patterns using a phase shift of 90°, but also, there are algorithms that are independent of the amount of phase shift[4-12]. Recent works have reported new methods and algorithms that go from the study of a single, two or more steps to get a phase recovery; nevertheless, they have to cover some requirements to be applied in order to work properly[13-18]. The application of these algorithms requires of a phase change in the reference beam. In this work, the change of phase comes directly from the excited object. The three-frame technique by Wyant et al, established in 1984[6], is applied to a selected group of fringe patterns coming from a HS-ESPI system, where a continuous wave laser illumination and a high speed camera are used.

* Corresponding author:
davidgh@cio.mx (David Asael Gutiérrez Hernández)
Published online at http://journal.sapub.org/mechanics

2. Experimental Setup and Object Description

Figure 1 shows an out-of-plane sensitive HS ESPI. The beam coming from a cw laser with 6-Watts maximum and 532 *nm*, is divided into an object beam and a reference beam, IO and IR respectively, by a beam splitter. The object beam is projected over the target by means of a 10x microscope objective and the reflection of this is recombined by a second beam splitter. The reference beam is re-directed to the second beam splitter and then to the sensor of the camera. For this experiment the laser is set to a power of 5.5 Watts, the exposure time of the CMOS camera is set at 4000 frames per second and the shutter is all the time open.

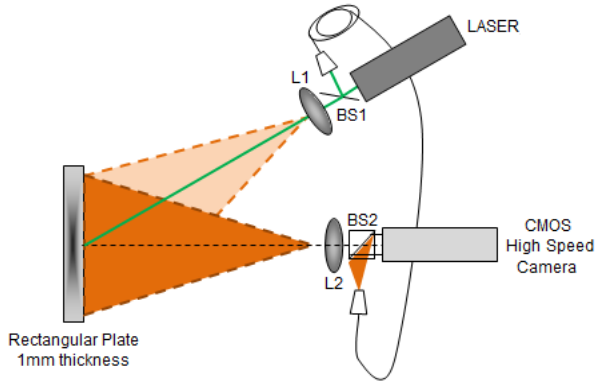

Figure 1. Optical set up for a high-speed ESPI system. Beam splitter 1 is a 70/30, beam splitter 2 is a 50/50, microscope objectives are 10x. The object to study is a 140x190x1 mm rectangular aluminum plate

A rectangular aluminum plate clamped in its four sides that carries a uniformly distributed load is the object to be studied. The plate is excited by an external sine wave generator placed behind it and plugged to a conventional speaker to generate vibration all over the plate. The first vibration modal for this plate is reported at 320 Hz[24]. The evolution of the vibration is recorded by a high-speed CMOS camera and having an image lens with a focal length of 75mm in order to get the whole object into the CMOS sensor.

The mechanical properties of the plate are mass density ρ = 2700 kg/m^3, Young's modulus E = 70 GPa and the Poisson ratio υ = 0.33. The geometric dimensions of the plate are Length L = 190 mm, width W = 140 mm and thickness h = 1 mm.

According to several authors, the equation for the vibrating rectangular plate is given by[19-23].

$$\partial^2 u/\partial t^2 = c^2\left(\partial^2 u/\partial x^2 + \partial^2 u/\partial y^2\right) \tag{1}$$

Where the deformation variable $u(x,y,t)$ must satisfy the border conditions $u = 0$ for all $t > 0$, c depends on the mechanical properties of the material of the plate. Eq. (1) can be solving by applying the variables separation method as the product of two functions of the form:

$$u(x,y,t) = F(x,y)G(t) \tag{2}$$

and again, applying the variables separation method $F(x,y)$ can be written as:

$$F(x,y) = H(x)Q(y) \tag{3}$$

After a mathematical procedure, the expression that gives the solution on function of the dimensions of the plate, a for the length, b for the width and for each horizontal and vertical vibration modal, w and z respectively is:

$$u_{wz}(x,y,t) = \left(B_{wz}\cos\lambda_{wz}t + B^*_{wz}\sin\lambda_{wz}t\right)\sin\left(w\pi/a\right)\sin\left(z\pi/b\right) \tag{4}$$

where

$$\lambda_{wz} = c\pi\sqrt{w^2 + z^2} \tag{5}$$

Figure (2) shows the principal numerical analysis of the rectangular plate.

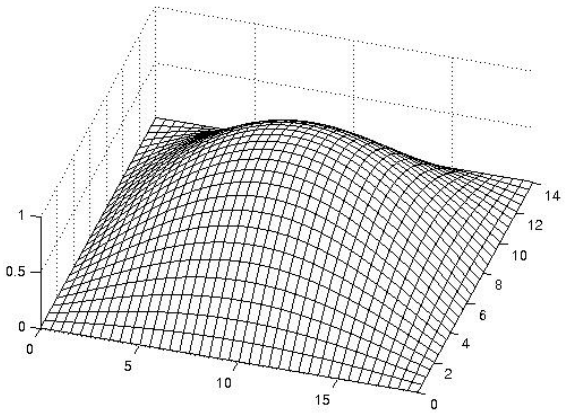

(a)

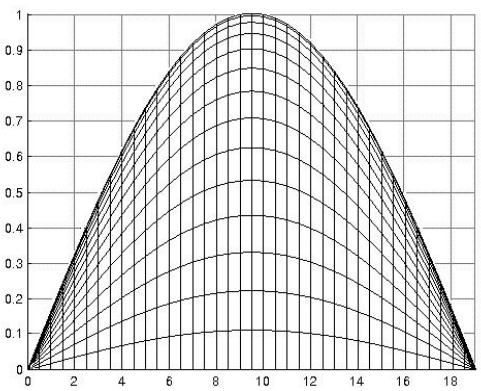

(b)

Figure 2. (a) Numerical model for the first vibration modal of the rectangular plate, (b) profile of the dynamic deformation of the plate in a = 19

The deformed profile of the vibrating plate on its first natural mode of frequency fits a polynomial function of degree 2 or 4.

3. Theoretical Description

In the high speed optical interferometry technique, the addition of the reference beam I_R and the object beam I_O is written as

$$I_1 = I_O + I_R + 2\sqrt{I_O I_R}\cos(\Psi) \quad (6)$$

where Ψ is the subtraction of the phase of the wavefront of the object beam ϕ_O and the reference beam ϕ_R.

Once the surface of the object is deformed, the phase of I_1 changes by $\Delta\phi$, and thus the sum of two beams after deformation I_2 can be written as

$$I_2 = I_O + I_R + 2\sqrt{I_O I_R}\cos(\Psi + \Delta\phi) \quad (7)$$

The subtraction of intensities of the input images I_1 and I_2 can be given by

$$I_1 - I_2 = 4\sqrt{I_O I_R}\sin\left(\psi + \frac{1}{2}\Delta\varphi\right)\sin\left(\frac{1}{2}\Delta\varphi\right) \quad (8)$$

Eq. (8) represents a fringe pattern that can be numerically processed to obtain a phase map for measuring the deformation of the object on a specific time.

When a sinusoidal signal produces an oscillated vibration on the surface of the object, the phase change $\Delta\phi$ can be expressed as

$$\Delta\phi = \frac{4\pi}{\Lambda} A\sin\omega t \quad (9)$$

where Λ is the wavelength of a laser, A is the amplitude and ω is the natural frequency.

Eq. (9) indicates that the vibration on the object's surface will change cyclically from a minimum until a maximum amplitude *A*. It is considered that in a HS-ESPI system there are more than two intensities that can be stored by a sensor while the object is under deflormation, $I_1, I_2, I_3, \ldots, I_n$, then, the phase of the intensity patterns of interference will change from $\Delta\phi = 0$ until 2π.

The number of intensity patterns of interference stored in a complete vibration cycle will depend on the natural frequency, ω, and on the exposure time of the CMOS camera, τ.

In this case, the intensity patterns of interference stored by the camera can be written as

$$I_n(x,y) = I_O(x,y) + I_R(x,y) + 2\sqrt{I_O(x,y)I_R(x,y)}\cos\left(\psi(x,y) + \frac{2(n-1)\pi}{m}\right) \quad (10)$$

where *m* is the number of intensity patterns of interference that can be obtained by the relation between the exposure time of the camera and the vibration frequency of the plate, it can be calculated from $m = \text{int}\left[\tau\omega^{-1}\right]$ and $n = 1, 2, 3, 4, 5, 6, \ldots, m$.

The integer function int[ ] gives an integer number of intensity patterns of interference that fit in a complete cycle of vibration conserving always the same amount of phase shifts between them.

The subtraction of intensities of the input images $|I_1 - I_2|$, $|I_2 - I_3|$, to $|I_n - I_m|$ can be given by

$$|I_{1..n}(x,y) - I_{2..m'}(x,y)| = |4\sqrt{I_O(x,y)I_R(x,y)}\sin\left(\begin{matrix}\psi(x,y)\\ +\frac{(n'-1)\pi}{m}\end{matrix}\right)\sin\left(\frac{(n'-1)\pi}{m}\right)| \quad (11)$$

$$|I_2(x,y) - I_{3..n'}(x,y)| = |4\sqrt{I_O(x,y)I_R(x,y)}\sin\left(\begin{matrix}\psi(x,y)\\ +\frac{(n'-1)\pi}{m}\end{matrix}\right)\sin\left(\frac{(n'-1)\pi}{m}\right)| \quad (11b)$$

$$|I_3(x,y) - I_{4..n'}(x,y)| = |4\sqrt{I_O(x,y)I_R(x,y)}\sin\left(\begin{matrix}\psi(x,y)\\ +\frac{(n'-1)\pi}{m}\end{matrix}\right)\sin\left(\frac{(n'-1)\pi}{m}\right)| \quad (11c)$$

$$|I_m(x,y) - I_{m+1..n'}(x,y)| = |4\sqrt{I_O(x,y)I_R(x,y)}\sin\left(\begin{matrix}\psi(x,y)\\ +\frac{(n'-1)\pi}{m}\end{matrix}\right)\sin\left(\frac{(n'-1)\pi}{m}\right)| \quad (11d)$$

Each of these subtractions represents a fringe pattern and each of these fringe patterns can be processed for extracting the corresponding phase map along the deformation of the object for a specific time of the complete cycle of vibration, *n'* goes from 2 to *n*-number of frames per second recorded by the high speed camera.

With this information, it is very possible to do the reconstruction of the deformation during a complete vibration cycle of the object.

One of the most important considerations of this technique is that the measurement can be started at any time; it is only needed to select an intensity pattern and make a subtraction of the following consecutive intensity patterns to it. It is not need of any kind of synchronization or any kind of carrier to do the measurement.

Some of the phase shifting techniques requires a particular and exact amount of phase change between consecutive intensity measurements in order to apply specific algorithms for phase calculation.

Wyant[6] presented in 1984 a technique of phase measurement which depends of the amount of phase shift between consecutive measurements equal to $\alpha = \pi/2$ (90°), yielding three equations,

$$I_1'(x,y) = I_0(x,y)\left[1 + \gamma(x,y)\cos\left(\varphi(x,y) - \alpha\right)\right] \quad (12)$$

$$I_2'(x,y) = I_0(x,y)\left[1 + \gamma(x,y)\cos\varphi(x,y)\right] \quad (13)$$

$$I_3'(x,y) = I_0(x,y)\left[1 + \gamma(x,y)\cos\left(\varphi(x,y) + \alpha\right)\right] \quad (14)$$

where the phase shift, α, is assumed to be linear. I_0 is the background intensity, γ is the fringe modulation, $\phi(x,y)$ is the phase distribution to be measured. From these equations, the phase at each point is

$$\phi(x,y)=\tan^{-1}\left[\left(\frac{1-\cos\alpha}{\sin\alpha}\right)\frac{I_1'-I_3'}{2I_2'-I_1'-I_3'}\right] \quad (15)$$

where

$$I_2'-I_3'=2I_0\gamma\sin\phi(x,y)\sin\alpha \quad (16)$$

$$2I_2'-I_1'-I_3'=2I_0\gamma\cos\varphi(x,y)(1-\cos\alpha) \quad (17)$$

The fringe modulation for this technique for the general phase shift α is

$$\gamma=\sqrt{\frac{[(1-\cos\alpha)(I_1'-I_3')]^2+[\sin(2I_2'-I_1'-I_3')]^2}{2I_0\sin\alpha(1-\cos\alpha)}} \quad (18)$$

$$\phi(x,y)=\tan^{-1}\left(\sqrt{3}\frac{I_1-I_3}{2I_2-I_1-I_3}\right) \quad (19)$$

It is important to notice that when $\alpha=2\pi/3$, eq. (15) can be written as and the detected fringe visibility for a $2\pi/3$ phase shift is

$$\gamma=\frac{\sqrt{3(I_1'-I_3')^2+(2I_2'-I_1'-I_3')^2}}{3I_0} \quad (20)$$

4. Simulating results

Consider a full resonant vibration cycle at ω = 320Hz, with the CMOS camera working at an exposure time, τ = 4000 fps. The relation of intensity patterns of interference recorded by the camera gives a sample of m=12 fringe patterns along the whole vibration event. The intensity patterns are separated from each other by a constant time.

To reach the 12 fringe pattern, we start from any intensity pattern of intensity at any time, called I_1, and then the subsequence intensity is subtracted from it, then, the followed intensity pattern, I_2 is selected and the subsequence intensity is subtracted from it, same procedure keeps doing until cover the full cycle of vibration according to eq. (11d). Then a selected fringe pattern is chosen for all the combinations and is used to be applied on the Wyant's algorithm.

The fringe patterns obtained by the subsequent subtraction of the intensity patterns are shown in figure 3. The figure represents a complete cycle of vibrating evolution where the maximum deformation of the plate is located in the center of it. In accordance to eq. (1) the deformation of the plate must follow a polynomial function of degrade 2 or 4.

According to Wyant, a single fringe pattern is selected and then shifted by a certain amount of phase in order to recover the phase of deformation. For this simulation the fringe pattern selected is the one inside the rectangle in figure 3 (b), Figure 4 shows the profile of the fringe patterns to be used in Wyant's algorithm.

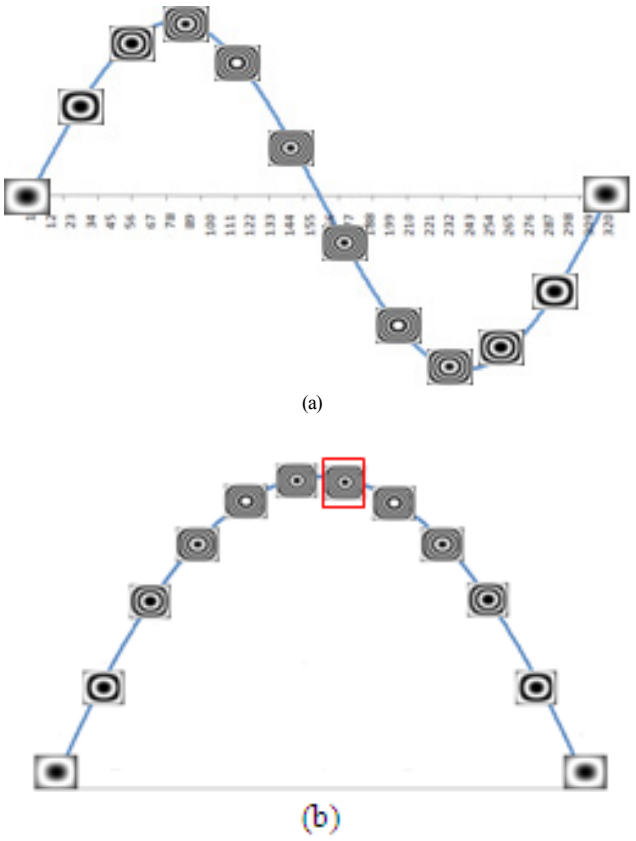

Figure 3. Representation of a full vibration cycle. (a) Optical phase change along the cycle. The y axis measures the relative deformation amplitude and the x axis shows the interferograms at different phase and time positions. (b) Each fringe pattern represents an instant of the mechanical phase of deformation of the plate

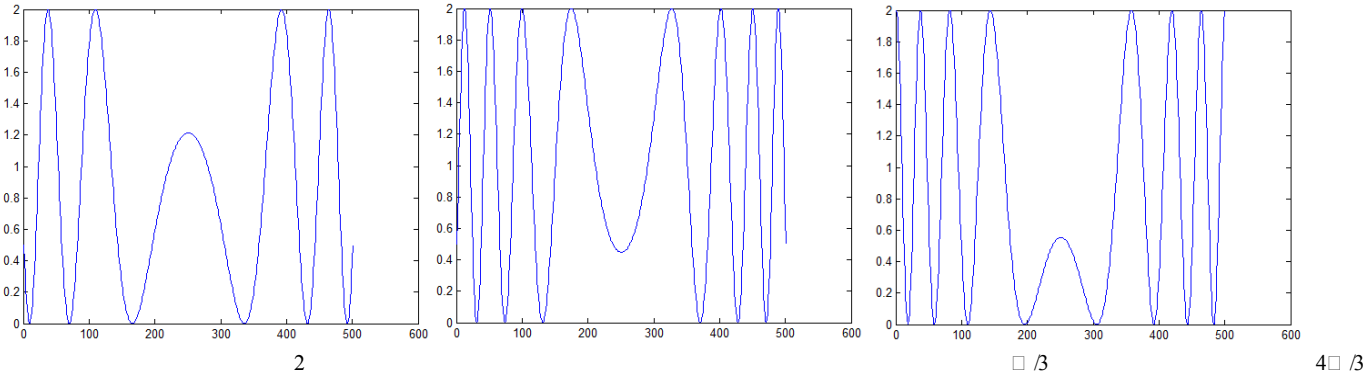

Figure 4. Shifted profiles of the selected fringe pattern

For this experiment these fringe patterns are separated from each other by the same amount of phase $\alpha = 2\pi/3$. Applying equation (19), the results are shown in Figure 5:

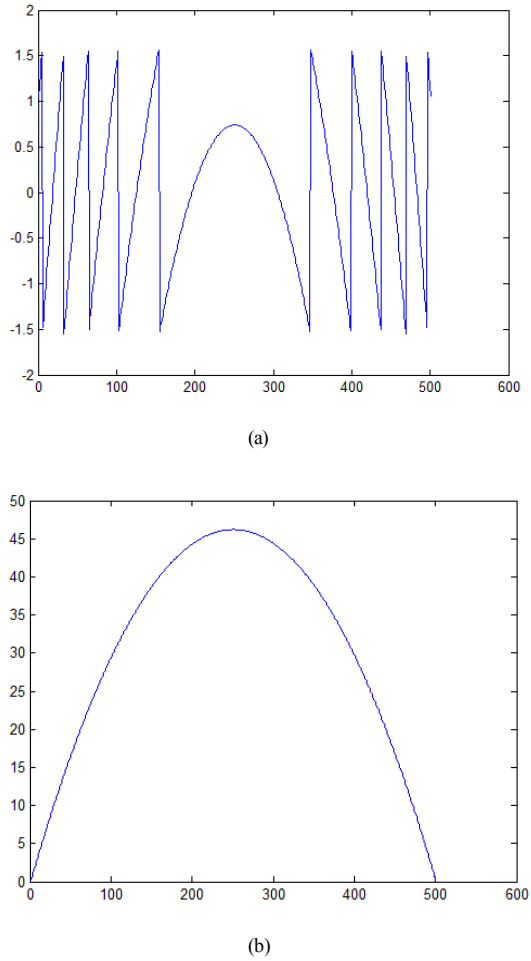

Figure 5. (a) Recovered phase of the rectangular plate under deformation; (b) Simulation of the profile of the deformation of the vibrating plate that comes from the processing of 3 selected fringe patterns with an amount of phase $\alpha_1=2\pi/3$ between each other

Figure 5 (b) shows the profile of the simulated plate measured along the center of it. The mathematical processing done in order to know the profile of the maximum deformation of the plate was done by applying software based on Matlab instructions.

5. Experimental Result

Figure 6 shows the intensity patterns of interference recorded by the HS ESPI.

The experimental fringe patterns coming by the HS-ESPI are shown in figure 7. This group of fringe patterns shows how the plate changes in a time interval of 0 to 250μs, 250μs to 500μs, 500μs to 750μs, 750μs to 1ms, 1ms to 1.25ms until covering the 3.125ms needed for a complete cycle of vibration.

It is observed that in each time interval, there is a set of fringe patterns with a visible change of the optical phase between them. Each time interval represents also a part of the mechanical phase evolution, in an instant of time and also along the time until 3.125ms that is the time needed to cover a full cycle of vibration.

Taking advantage of using a high speed system, it is possible to choose the fringe pattern with the maximum information about the mechanical deformation of the plate due to the sinusoidal vibration. By simple observation (that can be also done by simple computational software to be more precise) it is possible to select the fringe pattern coming from the subtraction $|I_8-I_9|$ as the fringe pattern with more information, from there, the selected fringe pattern to be used in Wyne's algorithm is $|I_8-I_9|$ and the respective fringe patterns containing more information coming from following cycles of vibration, as it is shown in figure 8. It is important to remember that the selected fringe pattern can be anyone along the cycle and also, within all the posible fringe patterns coming from the HS ESPI system.

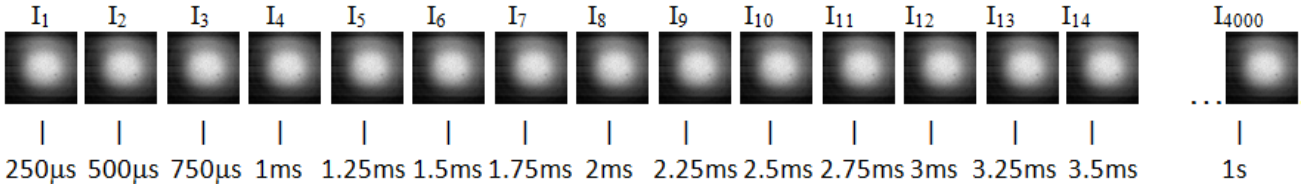

Figure 6. Intensity patterns of interference coming from the HS ESPI. Each of these images is separated by the same amount of phase from each other

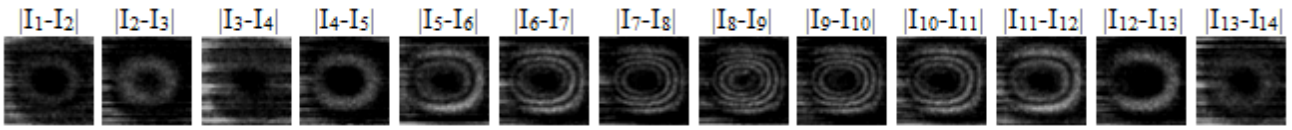

Figure 7. Fringe patterns coming from the subtraction of the intensity patterns of interference recorded by the HS ESPI system

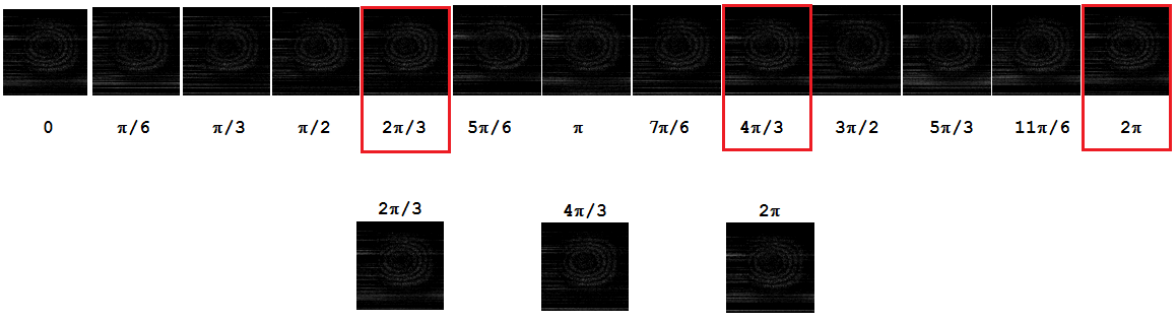

Figure 8. The selected fringe patterns to recover the mechanical profile of vibration of the plate

In Figures 7 and 8 there is a noise that looks like a group of horizontal lines. This phenomenon is due to manufacturing problems specifically for this model camera. According to the manufacturer, this error was corrected for subsequent versions. The camera's version is the NAC's Memrecam fx 6000, however, this phenomenon doesn't affect the measurement because it is a constant noise and not a phase changing.

Applying eqn. (19), the resulted phase is shown in figure 9.

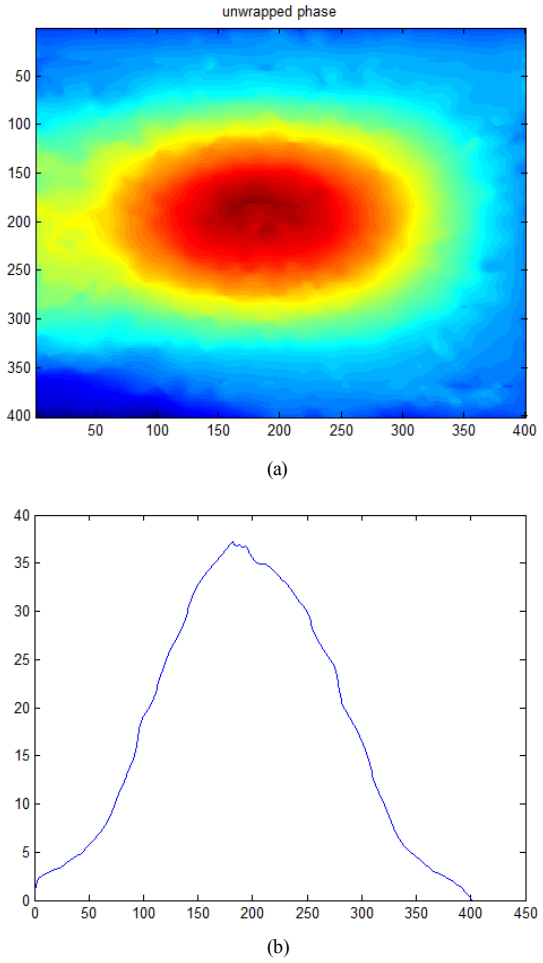

Figure 9. (a) Recovered phase of the experimental work; (b) Experimental profile of the maximum deformation of the rectangular plate that comes from the processing of 3 selected fringe patterns with an amount of phase $\alpha = 2\pi/3$ between each other. The x and y axis represent pixels and radians respectively

Figure 9 (b) shows the experimental profile measurement by the proposed method. Same as figure 6, figure 11 is measured along the center of the plate and it is shown that the profile fits a quadratic polynomial function just as the theory indicates. The maximum value of deformation shown in this graph could or couldn't represent the maximum deformation that the plate suffers in reality; y-axis represents the amplitude value on radians of the deformation, x-axis is in mm. For this experiment the adjustment of experimental results to a polynomial function of grade 4 is equal to 0.9953. It means that the experimental profile measured on this work fits the theory and also to the simulated profiles because it follows a polinomial function of grade 4. This adjustment indicates that the method works without the need of synchronization and without the need of mechanically tilt a component for shifting an amount of phase in the experiment.

As it is shown, by means of HS-ESPI, the mechanical amplitude that is resulted of the processing of the fringe patterns represents relative values of the profile that has been measured.

Selecting a different vibration frequency involves a different exposure time on the camera. We work at 320Hz because it is the first vibration natural mode of the rectangular plate and the relation mentioned on the manuscript between the exposure time and the vibration frequency give us enough fringe patterns that can be used in the proposed method and ensure that we can measure a complete vibration cycle. The second and third vibration natural modes are 540 Hz and 740 Hz respectively as they were found in[22].

It is important to notice that this profile could or couldn't exhibit the maximum deformation suffered by the plate. It is because the method employed in this work doesn´t need to be calibrated or synchronized.

6. Conclusions

A HS-ESPI system working with the Wyant's technique of phase shifting is a very fast way to measure maximum mechanical displacement. The introduction of a high speed camera to an ESPI set up eliminates the need for tilted mirrors or piezoelectric devices for obtaining the phase and also eliminates the need of electronically synchronization.

High speed cameras and continuous wave lasers give a very strong way for measuring real time vibrations; it can be a very interesting solution to be applied in industry. The system records a sequence of 4000 fps, which can be use for applying some of the phase shifting techniques proposed from many authors and can be useful to characterize the complete vibration evolution of a dynamic event. HS ESPI is a technique that allows a very fine exploration of mechanical displacements considering either static or dynamic events. The most important issue of the technique corresponds to a non contact and non invasive measurements.

ACKOWLEDGMENTS

The authors would like to acknowledge partial financial support from Consejo Nacional de Ciencia y Tecnología, Grant 48177.

REFERENCES

[1] U. Schnars, "Direct phase determination in holographic interferometry with use of digitally recorded holograms", Opt. Soc. Am. A, 11, 2011-2015, (1994).

[2] T. M. Kreis, W. P. O. Jüptner, "Principles of Digital Holography", Fringe ´97 Proc. of the 3rd international workshop on automatic processing of fringe patterns, 353-363 (1997).

[3] C. Pérez-López, F. Mendoza Santoyo, and M. de la Torre Ibarra, "Low level free vibration measurements using high speed digital holography", Proc. AIP 992, 810 -815 (2007).

[4] P. Carré, "Installation et utilisation du comparateur photoélectrique et interferentiel du Bureau International des Poids et Mesures," Metrologia **2**(1), 13–23 (1966).

[5] M. Takeda, H. Ina, and S. Kobayashi, "Fourier-transform method of fringe-pattern analysis for computer-based topography and interferometry," J. Opt. Soc. Am. 72(1), 156–160 (1982).

[6] J. C. Wyant, *C.* L. Koliopoulos, B. Bhushan, and O. E. George, ″An Optical Profilometer for Surface Characterization of Magnetic Media,″ ASLE Trans. 27, 101–113 (1984)

[7] Y. Y. Cheng, and J. C. Wyant, "Phase shifter calibration in phase-shifting interferometry," Appl. Opt. 24(18), 3049–3052 (1985).

[8] P. Hariharan, "Digital phase-shifting interferometry : a simple error compensating phase calculation algorithm," Appl. Opt. 26, 2504-0505 (1987).

[9] C. Roddier, and F. Roddier, "Interferogram analysis using Fourier transform techniques," Appl. Opt. 26(9), 1668–1673 (1987).

[10] K. Creath, "Phase-measurement interferometry techniques," Progress in Optics, 26, 350-393, E. Wolf, ed., North Holland, Amsterdam (1988).

[11] D. Kerr, F. Mendoza Santoyo, and J. R. Tyrer, "Extraction of phase data from electronic speckle pattern interferometric fringes using a single-phase-step method: a novel approach," J. Opt. Soc. Am. A, 7, 820-826 (1990).

[12] K. A. Goldberg, and J. Bokor, "Fourier-transform method of phase-shift determination," Appl. Opt. 40(17), 2886–2894 (2001).

[13] Q. Yu, S. Fu, X. Liu, X. Yang, and X. Sun, "Single-phase-step method with contoured correlation fringe patterns for ESPI," Opt. Express 12(20), 4980–4985 (2004).

[14] J. A. Quiroga, J. A. Gómez-Pedrero, M. J. Terrón-López, M. Servin, "Temporal demodulation of fringe patterns with sensitivity change", Optics Communications, 253, 266–275, (2005).

[15] X. H. Zhong, "Phase-step calibration technique based on a two-run-times-two-frame phase-shift method," Appl. Opt. 45(35), 8863–8869 (2006).

[16] Hyun-Jin Lee and Sang-Keun Gil, "Error Analysis for Optical Security by means of 4-Step Phase-Shifting Digital Holography," J. Opt. Soc. Korea 10, 118-123 (2006).

[17] Fuzhong Bai and Changhui Rao. "Phase-shifts nπ/2 calibration method for phase-stepping interferometry", Optics Express. 17(19), 16861-16868 (2009).

[18] Seok-Hee Jeon and Sang-Keun Gil, "2-step Phase-shifting Digital Holographic Optical Encryption and Error Analysis," J. Opt. Soc. Korea 15, 244-251 (2011).

[19] D. Young. "Analysis of clamped rectangular plates". Journal of Applied Mechanics, 62, A139-A142 (1940).

[20] T. H. Evans. "Tables of moments and deflections for a rectangular plate fixed on all edges and carrying a uniformly distributed load". Journal of Applied Mechanics, 61, A7-A10 (1939).

[21] I. A. Wojtaszak. "The calculation of maximum deflection, moment, and shear for uniformly loaded rectangular plate with clamped edges". Journal of Applied Mechanics, 59, A173-A176 (1937).

[22] S. P. Timoshenko. "Bending of rectangular plates with clamped edges". In Proceedings Fifth International Congress of Applied Mechanics, pages 40-43, Massachusetts Institute of Technology (1938).

[23] C. E. Imrak and I. Gerdemeli. "An exact solution for the deflection of a clamped rectangular plate under uniform load". Applied mathematical sciences, 1, 43, 2129-2137 (2007).

[24] A. Moore and C. Pérez-López. "Low-frequency harmonic vibration analysis with double-pulsed addition electronic speckle pattern interferometry". Opt. Eng. 35, **9**, 2641–2650 (1996).